Molecular Engineering to Introduce Carbonyl Between Nickel Salophen Active Sites to Enhance Electrochemical CO_2 Reduction to Methanol

Zhifu Liang[+], Jianghao Wang[+], Pengyi Tang[+], Weiqiang Tang[+], Lijia Liu, Mohsen Shakouri, Xiang Wang, Jordi Llorca, Shuangliang Zhao, Marc Heggen, Rafal E. Dunin-Borkowski, Andreu Cabot*, Hao Bin Wu*, Jordi Arbiol**

Z.F. Liang, Prof. J. Arbiol
Catalan Institute of Nanoscience and Nanotechnology (ICN2), CSIC and BIST
Campus UAB, Bellaterra, 08193 Barcelona, Catalonia, Spain
Email:arbiol@icrea.cat

Dr. J. H. Wang
Institute of Zhejiang University - Quzhou, 78 Jiuhua Boulevard North, Quzhou 324000, China
Email: wjh7744@zju.edu.cn

Prof. P. Y. Tang
Institute of Microsystem and Information Technology, Chinese Academy of Sciences, Shanghai 200050, China

Z.F. Liang, X. Wang, Prof. A. Cabot
Catalonia Institute for Energy Research - IREC
Sant Adrià de Besòs, Barcelona, 08930, Catalonia, Spain
Email: acabot@irec.cat

Prof. L. Liu
Department of Chemistry, Western University, 1151 Richmond Street, London, ON N6A5B7 Canada

Prof. H. B. Wu
Institute for Composites Science Innovation (InCSI), School of Materials Science and Engineering, Zhejiang University, Hangzhou 310027, China
Email: hbwu@zju.edu.cn

Dr. W. Tang, Prof. S. L. Zhao
State Key Laboratory of Chemical Engineering and School of Chemical Engineering, East China University of Science and Technology, Shanghai, 200237, China

Prof. P. Y. Tang, Dr. M. Heggen, Prof. R. E. Dunin-Borkowski
Ernst Ruska-Centre for Microscopy and Spectroscopy with Electrons and Peter Grünberg Institute Forschungszentrum Jülich GmbH 52425 Jülich, Germany

Prof. J. Llorca
Institute of Energy Technologies, Department of Chemical Engineering and Barcelona Research Center in Multiscale Science and Engineering
Universitat Politècnica de Catalunya, EEBE, 08019 Barcelona, Catalonia Spain.

Dr. M. Shakouri
Canadian Light Source, Saskatoon, S7N 0X4, Canada

Prof. S. L. Zhao

Guangxi Key Laboratory of Petrochemical Resource Processing and Process Intensification Technology, School of Chemistry and Chemical Engineering, Guangxi University, Nanning, 530004, China

Prof. A. Cabot, Prof. J. Arbiol
ICREA
Pg. Lluís Companys 23, 08010 Barcelona, Catalonia, Spain

[+] These authors contribute equally to this work

* Corresponding authors

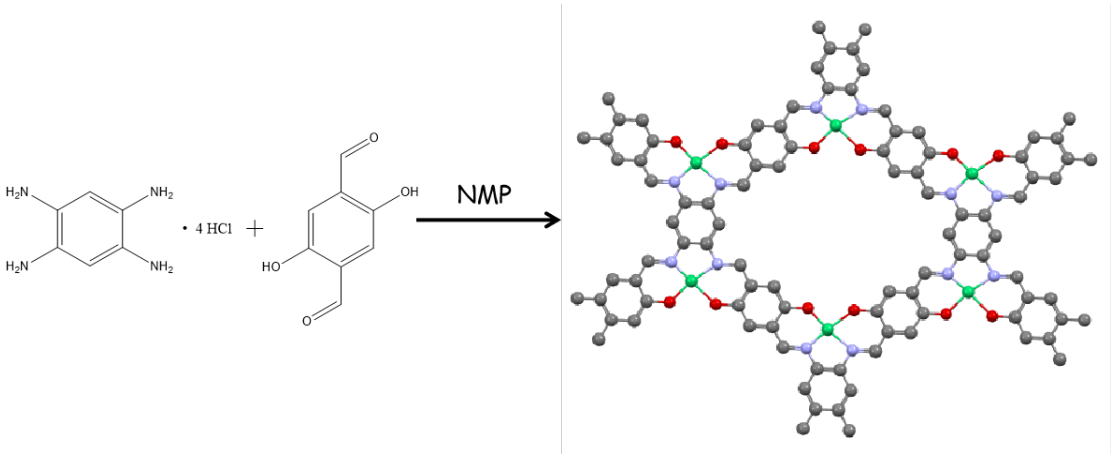

Figure S1. Synthesis scheme of Ni-2D-SA

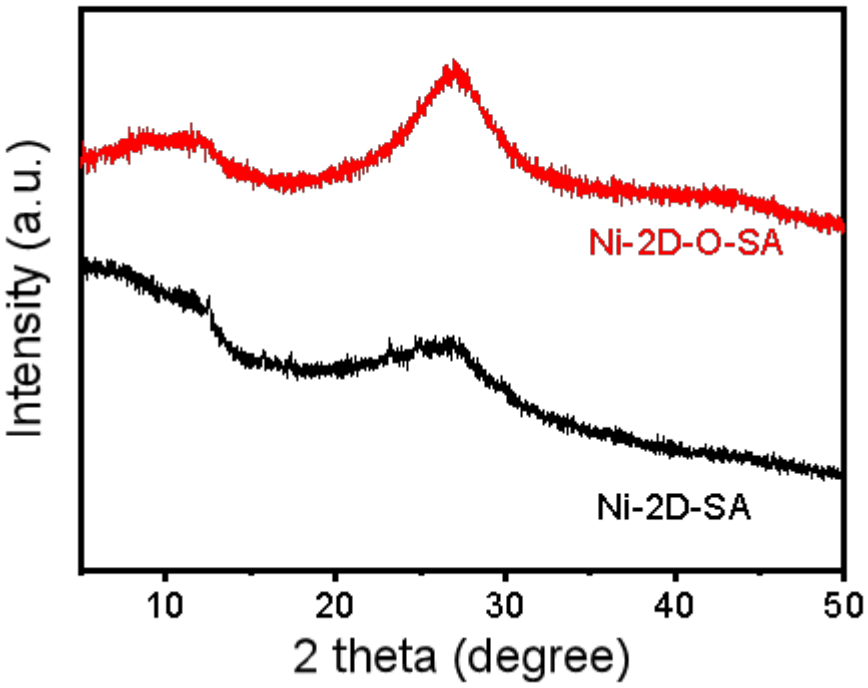

Figure S2. PXRD patterns of Ni-2D-SA (black) and Ni-2D-O-SA (red)

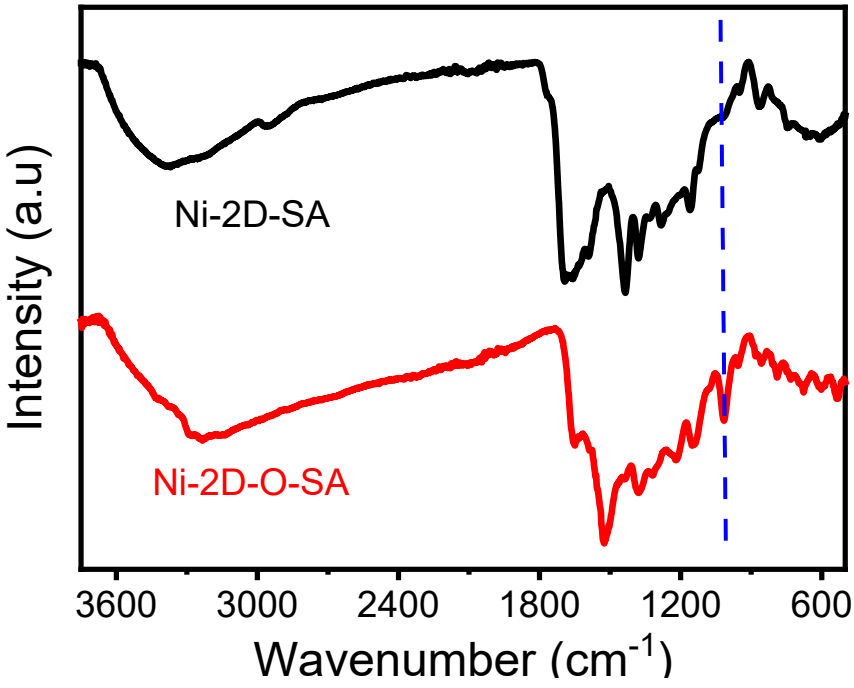

Figure S3. FT-IR spectra of Ni-2D-SA and Ni-2D-O-SA

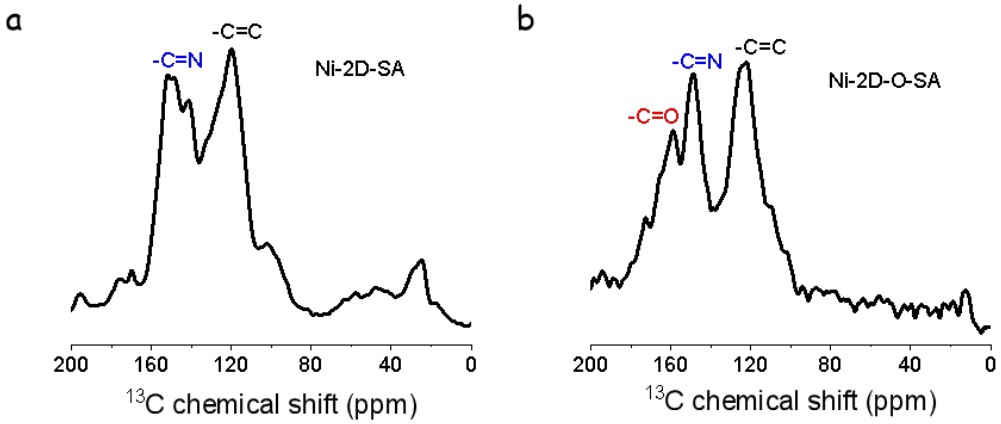

Figure S4. chemical shift of ^{13}C SSNMR spectra of Ni-2D-SA and Ni-2D-O-SA

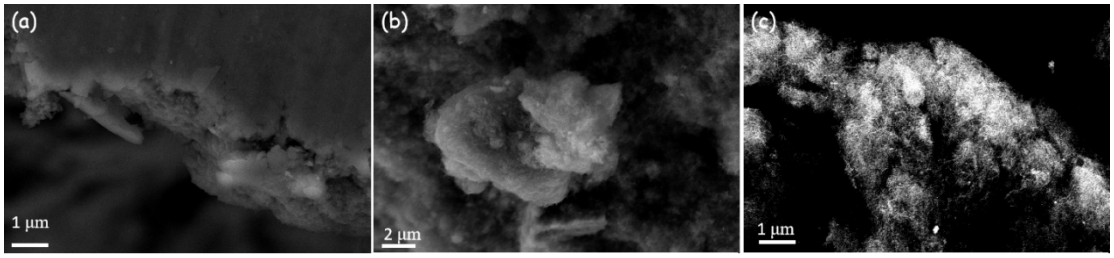

Figure S5 SEM images of: (a) Ni-2D-O-SA, (b) Ni-2D-O-SA-CNT, (c) Ni-2D-SA-CNT.

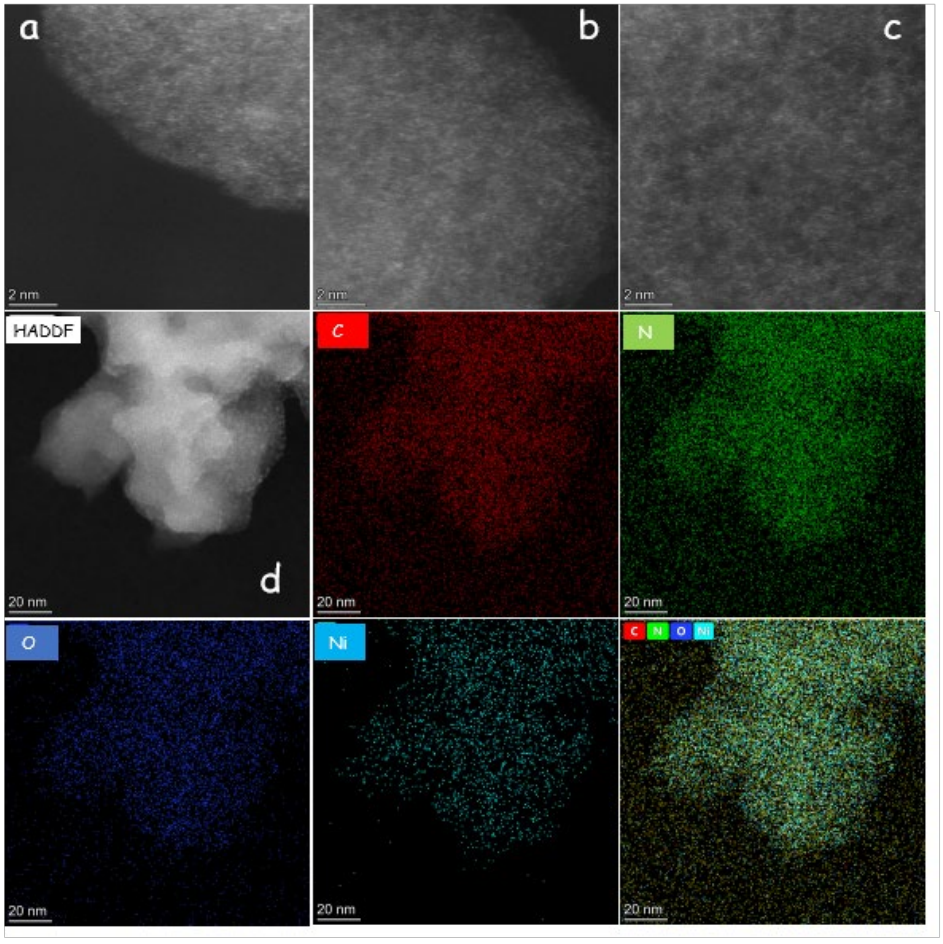

Figure S6. (a)-(c) HAADF-STEM images of Ni-2D-O-SA displaying the presence of atomically dispersed nickel atoms. (d) HAADF-STEM image and EDS mapping.

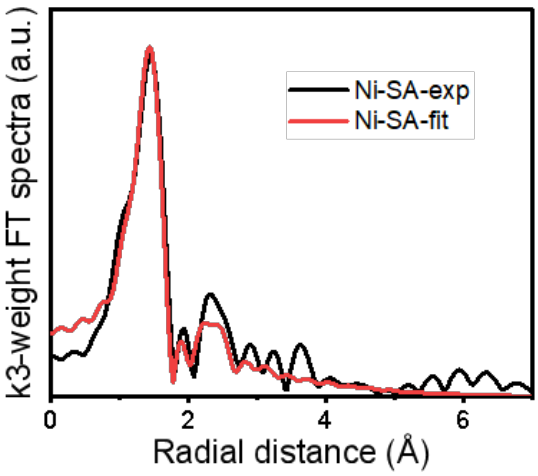

Figure S7. Fourier transformed Ni K-edge EXAFS spectra of Ni-SA plotted in R-space, Fourier transformed EXAFS spectra in R-space of Ni-SA and fitted curve.

Sample	**Bond**	**R(Å)**	**CN**	**σ^2 (10^{-3} Å^2)**	**ΔE (eV)**	**R factor**
Ni-SA	Ni-O	1.871 (0.015)	2	2 (1)	4.04 (1.49)	0.03
	Ni-N	1.820 (0.014)	2	2(1)		
	Ni...C	2.799 (0.029)	6	10 (4)		

Table S1. The Ni K-edge EXAFS fitting parameters of Ni-SA. R：bond length, CN: coordination number.

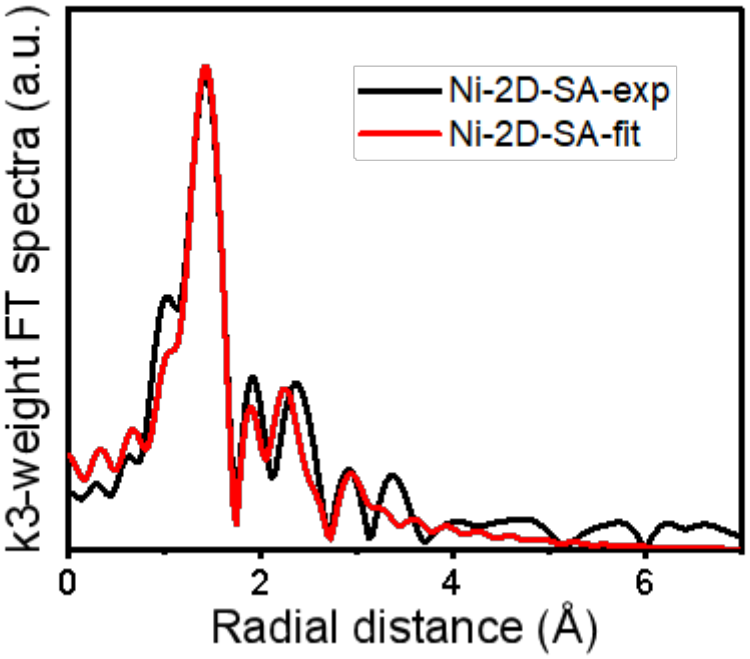

Figure S8. Fourier transformed Ni K-edge EXAFS spectra of Ni-2D-SA plotted in R-space, Fourier transformed EXAFS spectra in R-space of Ni-SA and fitted curve.

Table S2. The Ni K-edge EXAFS fitting parameters of Ni-2D-SA.

Sample	**Bond**	**R(Å)**	**CN**	**σ^2 (10^{-3} Å^2)**	**ΔE (eV)**	**R factor**
Ni-2D-SA	Ni-O	1.844 (0.015)	2	1 (1)	5.04 (1.52)	0.03
	Ni-N	2.070 (0.168)	2	30 (15)		
	Ni...C	2.760 (0.062)	6	11 (6)		
	Ni...Ni	3.170 (0.091)	1	11 (10)		

Table S3. The Ni K-edge EXAFS fitting parameters of Ni-2D-O-SA.

Sample	Bond	R(Å)	CN	σ^2 (10^{-3} Å^2)	ΔE (eV)	R factor
Ni-2D-O-SA	Ni-O	1.855 (0.024)	2	3 (1)	-4.93 (1.53)	0.02
	Ni-N	2.084 (0.031)	2	4 (3)		
	Ni...C	2.651 (0.052)	6	15 (4)		
	Ni...Ni	3.168 (0.043)	1	10 (5)		

R：bond length, CN: coordination number

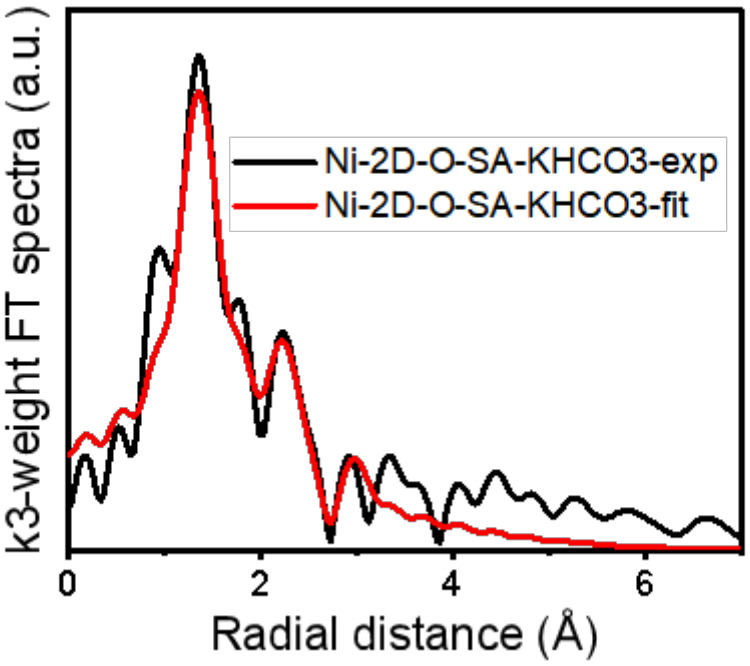

Figure S9. Fourier transformed Ni K-edge EXAFS spectra of Ni-2D-O-SA after immersed in $KHCO_3$ for three days plotted in R-space, Fourier transformed EXAFS spectra in R-space of Ni-SA and fitted curve.

Table S4. The Ni K-edge EXAFS fitting parameters of Ni-2D-O-SA-$KHCO_3$.

Sample	Bond	R(Å)	CN	σ^2 (10^{-3} Å^2)	ΔE (eV)	R factor
Ni-2D-O-SA-$KHCO_3$	Ni-O	1.995 (0.021)	2	3 (1)	3.35 (1.82)	0.02
	Ni-N	1.851 (0.018)	2	2 (2)		
	Ni...C	2.790 (0.035)	6	15 (3)		
	Ni...Ni	3.188 (0.050)	1	13 (7)		

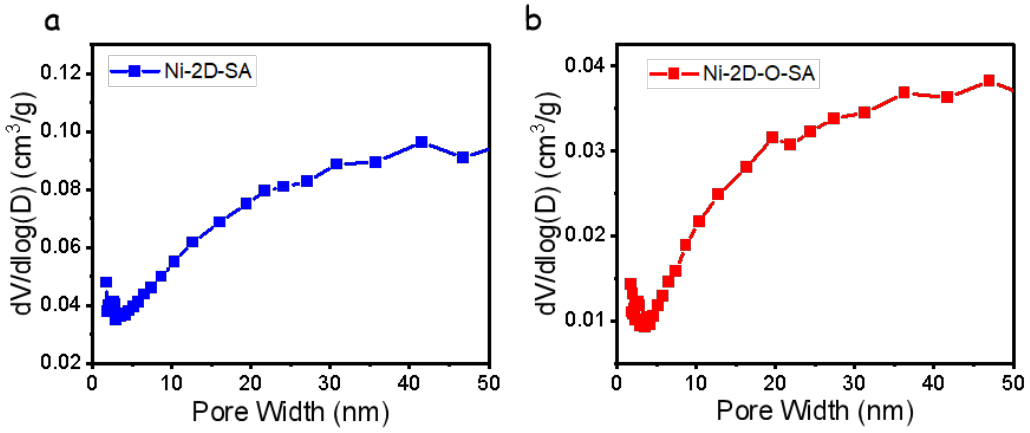

Figure S10. Pore size distribution of Ni-2D-SA and Ni-2D-O-SA powder, respectively.

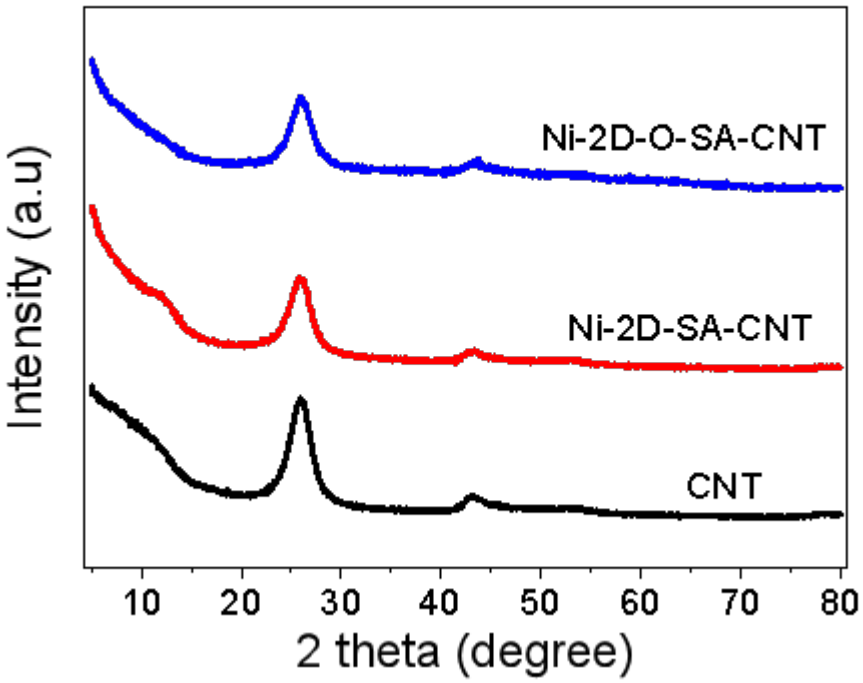

Figure S11. PXRD of Ni-2D-SA-CNT, Ni-2D-O-SA-CNT and CNT

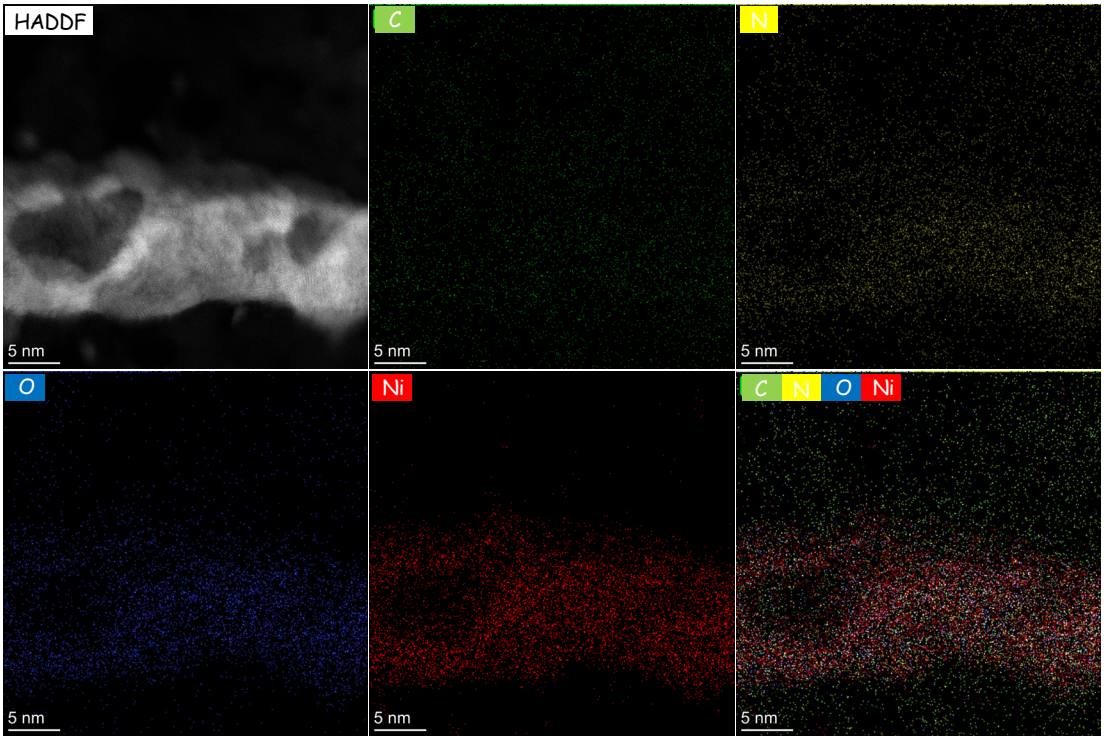

Figure S12. HAADF-STEM image and EDS elemental mapping for Ni-2D-O-SA-CNT.

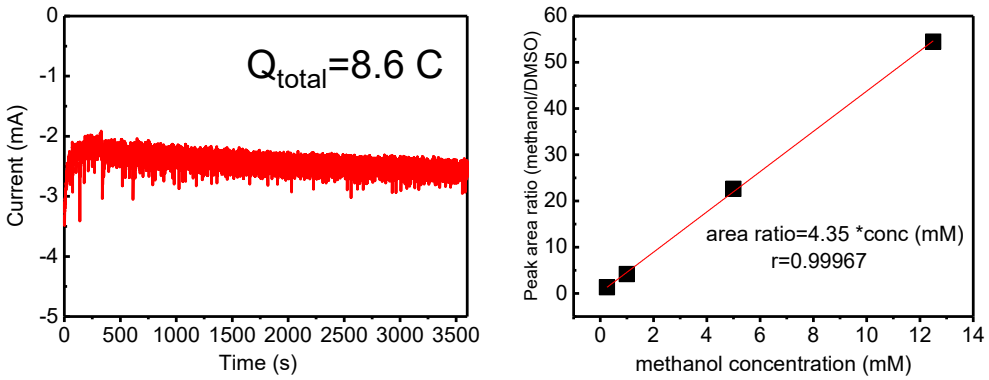

Figure S13. Left panel: i-t curve on Ni-2D-O-SA-CNT at -0.9 V vs. RHE for 1h

Right panel: Calibration curves for methanol (0.2 mM DMSO as internal standard)

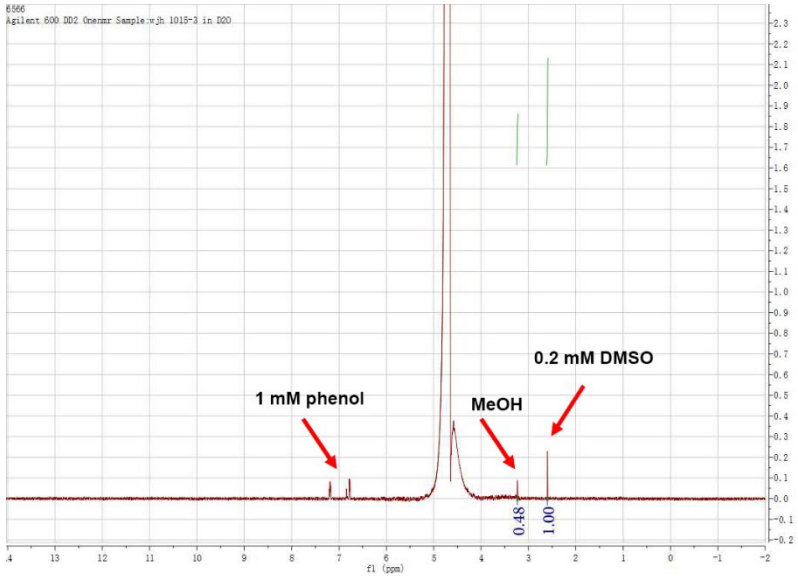

Figure S14. NMR spectrum of the catholyte after 1 hour of CO2 reduction on Ni-2D-O-SA-CNT. Potential applied=-0.9 V vs RHE. The peak located at 3.23 ppm is the signal of methanol.

The peaks were quantified by integrating the area. the relative peak area can be calculated as follows:

$$\text{Relative peak area ratio (methanol)} = \frac{\text{singlet peak area at 3.23ppm (methanol)}}{\text{singlet peak area at 2.6 ppm (DMSO)}}$$

$$FE_{methanol} = \frac{\frac{0.48}{4.35} * 10^{-3} * 0.035 * 6.02 * 10^{23} * 6e}{\frac{8.6}{1.602 * 10^{-19} e}} * 100\% = 25.9\%$$

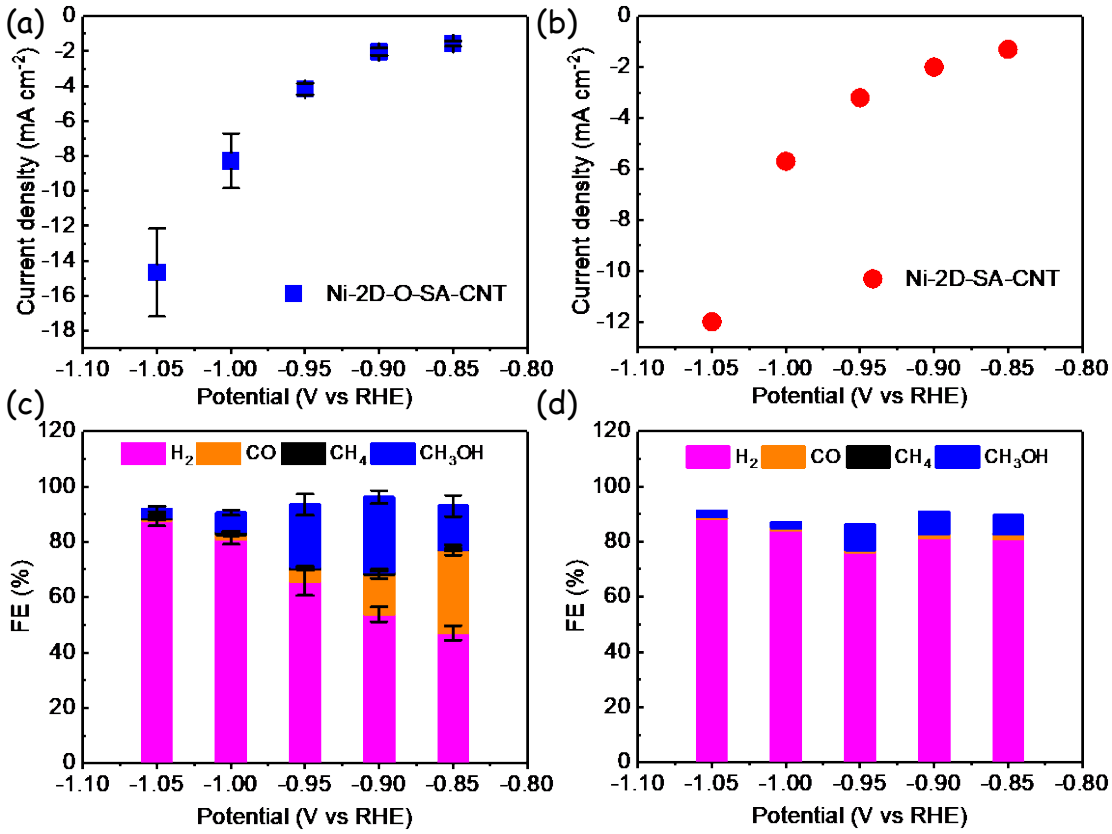

Figure S15. (a and b) Current densities of CO_2RR for Ni-2D-O-SA-CNT and Ni-2D-SA-CNT at various potentials. (c and d) Product distribution of CO2RR for Ni-2D-O-SA-CNT and Ni-2D-SA-CNT at various potentials.

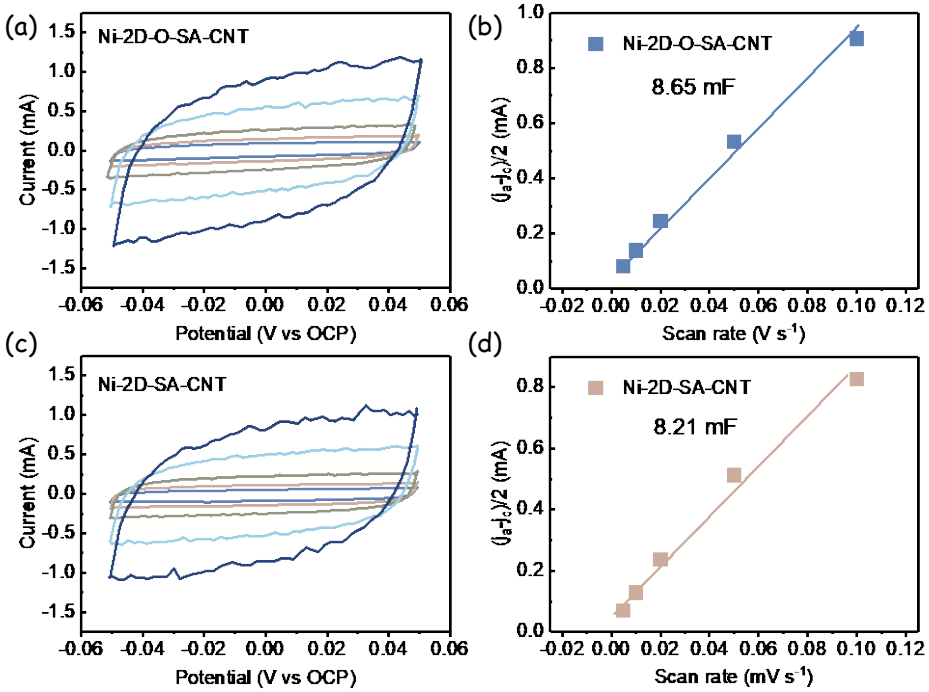

Figure S16. (a,c) CV curves on Ni-2D-O-SA-CNT and Ni-2D-SA-CNT with different scan rates (5, 10, 20, 50, 100 mV s^{-1}). (b, d) Current at open circuit potential (OCP) versus scan rates of different samples. The electrode area is 1 cm^{-2}.

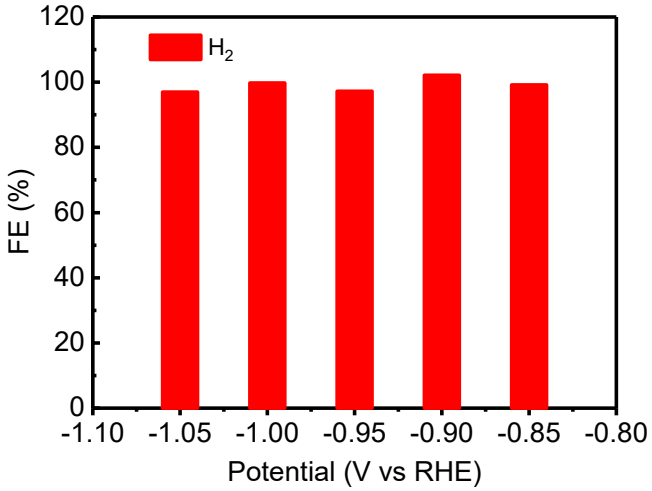

Figure S17. Product distribution for Ni-2D-O-SA-CNT under Ar-saturated 0.1 M $KHCO_3$ electrolyte at various potentials.

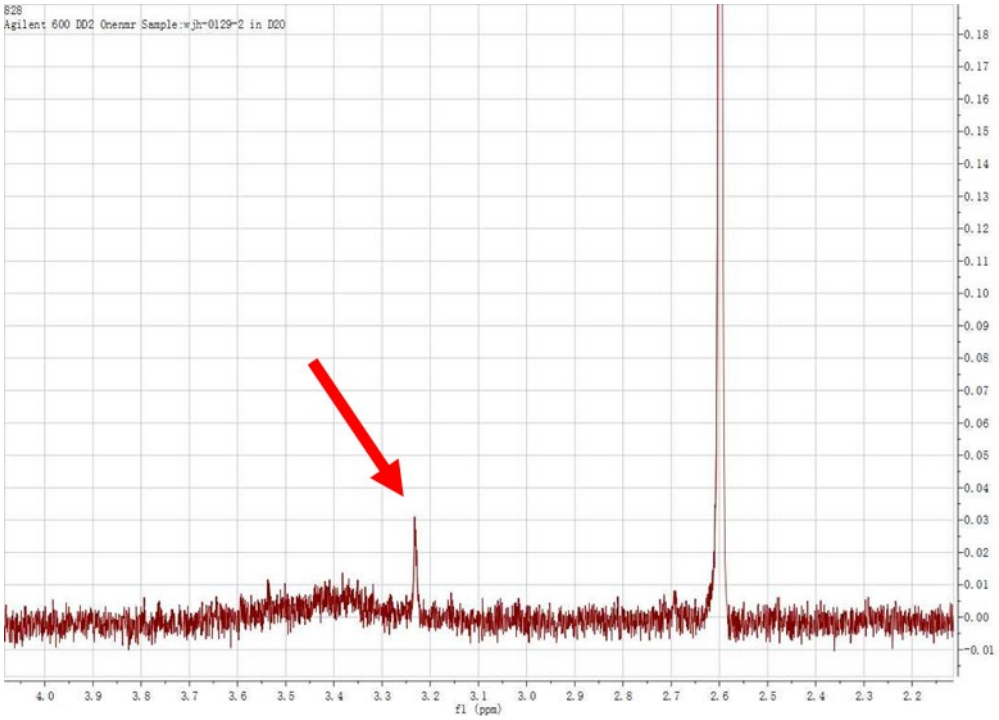

Figure S18. NMR spectrum of the catholyte after 1 hour of CO_2 reduction on Ni-2D-O-SA-CNT. Potential applied=-0.9 V vs RHE. The peak located at 3.23 ppm is the signal of methanol.

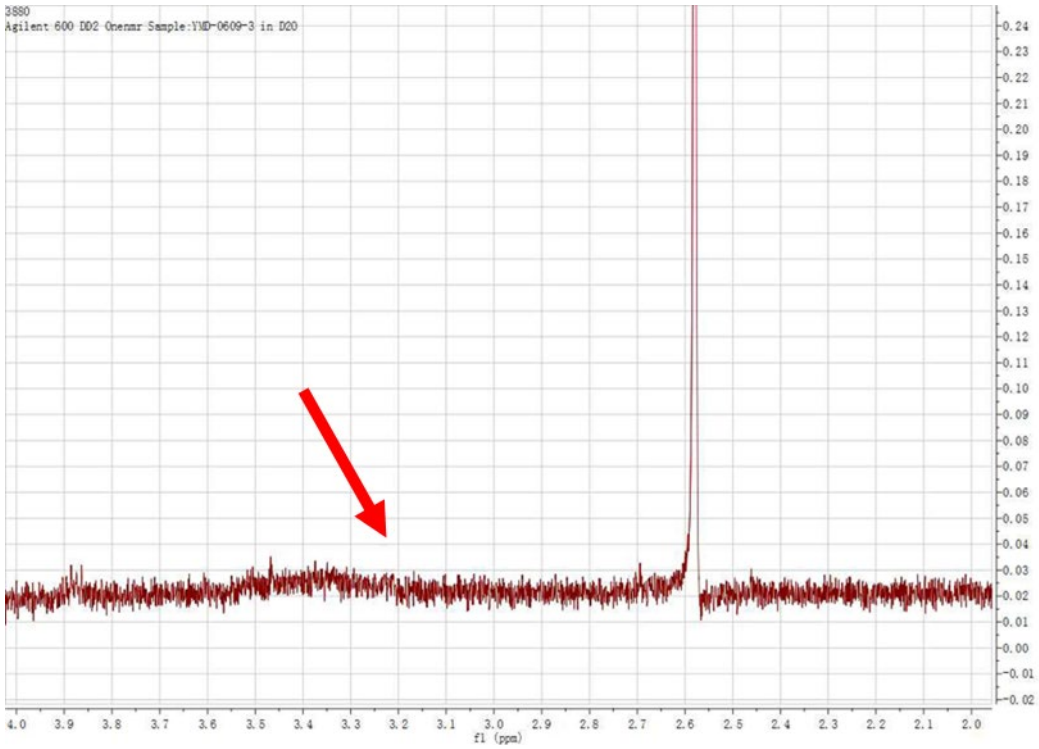

Figure S19. NMR spectrum of the catholyte after 1 hour of electro-reduction under Ar environment on Ni-2D-O-SA-CNT. Potential applied=-0.9 V vs RHE.

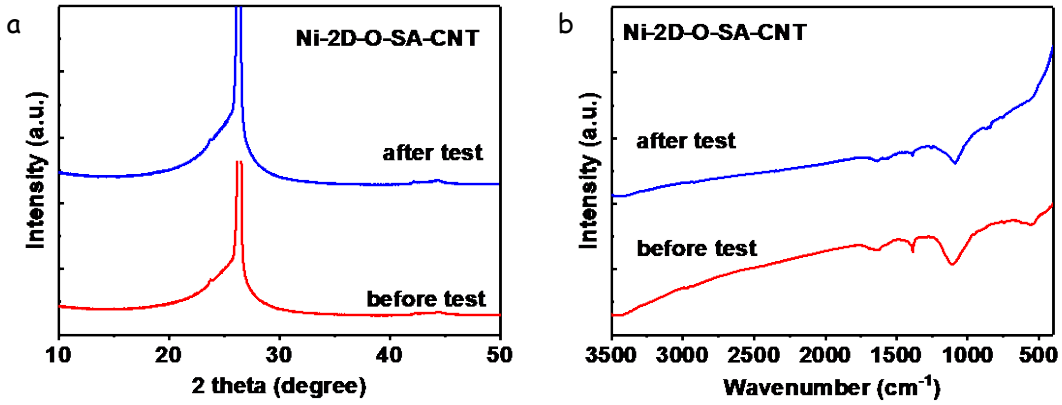

Figure S20. (a) XRD patterns and (b) FT-IR spectra of Ni-2D-O-SA-CNT on carbon paper before and after 1 hour of CO_2RR test.

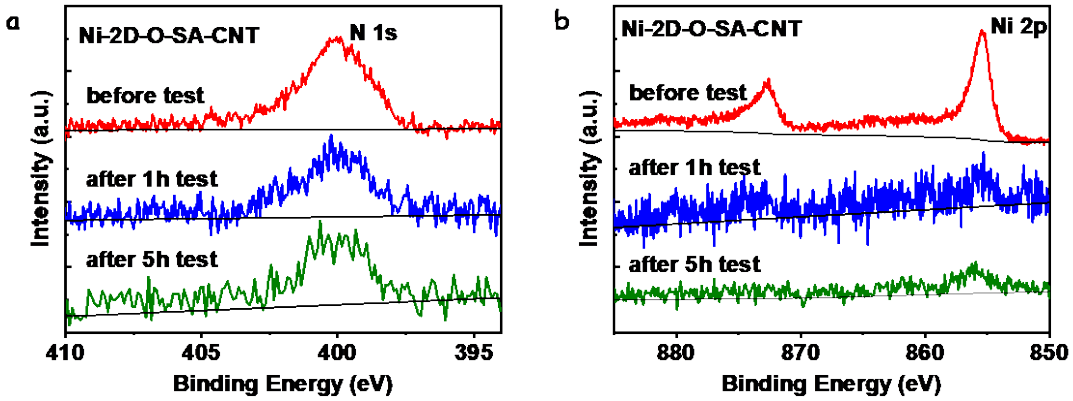

Figure S21. XPS spectra of Ni-2D-O-SA-CNT on carbon paper before and after 1 and 5 hours of CO_2RR test.

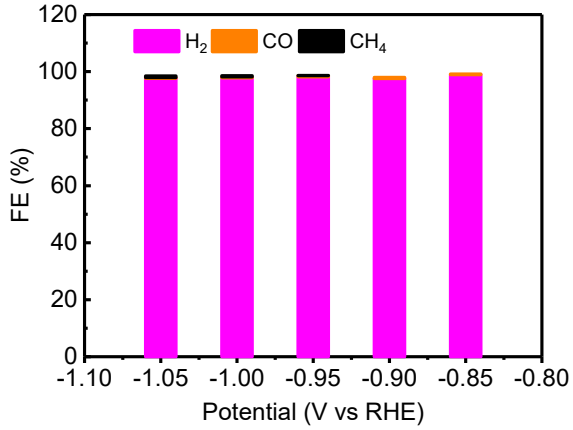

Figure S22. Product distribution of CO_2RR for 2D-O-SA-CNT (without nickel) at various potential.

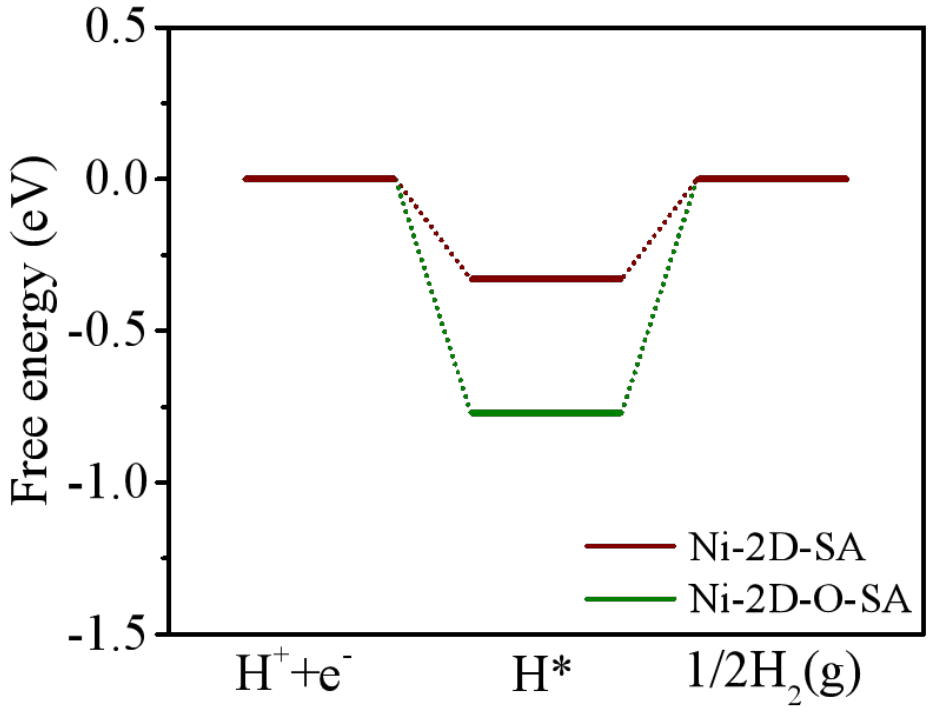

Figure S23. Free-energy profiles of hydrogen evolution reaction (HER) on selected segments of Ni-2D-SA and Ni-2D-O-SA, respectively.

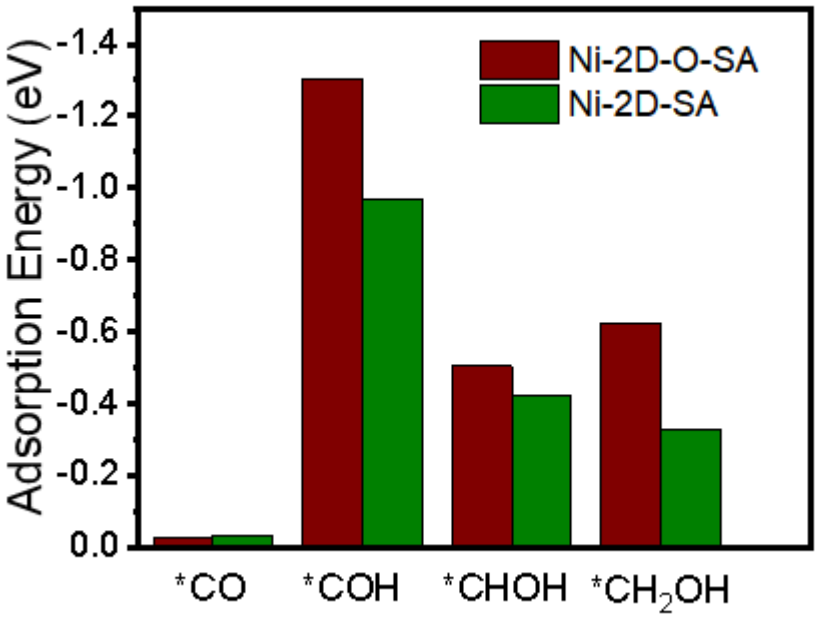

Figure S24. The adsorption energy for intermediates (from CO to methanol) on selected segments of Ni-2D-SA and Ni-2D-O-SA, respectively.

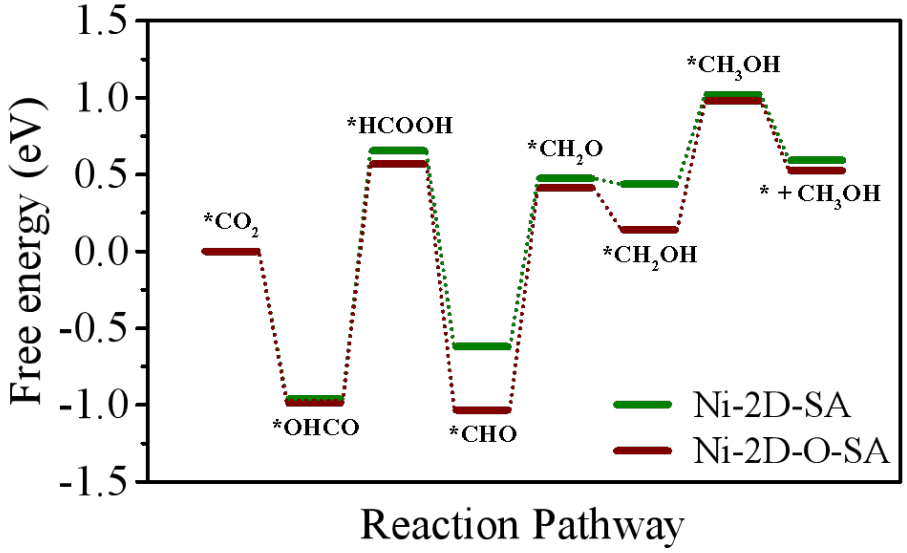

Figure S25. Free energy diagram of CO_2 to CH_3OH on selected segments of Ni-2D-O-SA.

Table S5. Performance comparison of our catalysts and previous reported molecular based electrocatalysts for conversion of CO_2 to methanol

Catalysts	j_{CH3OH} (mA/cm^2)	Electrolyte Solution	Potential (vs RHE)	Faradaic Efficiency (%)	Ref.
Ni-2D-O-SA-CNT	**~ 0.7**	**0.1 M $KHCO_3$**	**-0.9 V**	**29.5**	**This work**
Ni-2D-SA-CNT	**0.28**	**0.1 M $KHCO_3$**	**-0.95 V**	**9.2**	**This work**
CoPc/CNT	10.6	0.1 M $KHCO_3$	-0.94 V	44	S1
CoPc-NH2/CNT	10.2	0.1 M $KHCO_3$	-1.00 V	32	S1
Mixture of CoPc and CNT	0.03	0.5 M $KHCO_3$	- 0.88 V	0.3	S2
$Cu_3(HHTQ)_2$	0.27	0.1 M $KHCO_3$	-0.4 V	53.6	S2
$Ni_3(HHTQ)_2$	/	0.1 M $KHCO_3$	-0.4 V	0.54	S3
$Cu_3(HHTP)_2$	/	0.1 M $KHCO_3$	-0.4 V	0.15	S3

References

[S1] Y. Wu, Z. Jiang, X. Lu, et al. Domino electroreduction of CO_2 to methanol on a molecular catalyst, Nature 575 (2019), 639-642.

[S2] E. Boutin, M. Wang, J.C. Lin, M. Mesnage, D.Mendoza, B. Lassalle-Kaiser, C. Hahn, T. F. Jaramillo, M. Robert, Aqueous Electrochemical Reduction of Carbon Dioxide and Carbon Monoxide into Methanol with Cobalt Phthalocyanine, Angew. Chem. Int. Ed. 58 (2019), 16172-16176.

[S3] J. Liu, D. Yang, Y. Zhou, G. Zhang, G. Xing, Y. Liu, Y. Ma, O. Terasaki, S. Yang, L. Chen, Tricycloquinazoline-Based 2D Conductive Metal-Organic Frameworks as

Promising Electrocatalysts for CO_2 Reduction. Angew. Chem. Int. Ed. Engl. 60 (2021), 14473-14479.